Int J Earth Sci (Geol Rundsch) (2017) 106:171–183
DOI 10.1007/s00531-016-1309-0

ORIGINAL PAPER

Steps in the intensification of Benguela upwelling over the Walvis Ridge during Miocene and Pliocene

Sebastian Hoetzel[1] · Lydie M. Dupont[1] · Fabienne Marret[2] · Gerlinde Jung[1] · Gerold Wefer[1]

Received: 15 September 2015 / Accepted: 16 February 2016 / Published online: 12 March 2016

Abstract Upwelling is a significant part of the ocean circulation controlling largely the transport of nutrient-rich cold waters to the surface and therefore influencing ocean productivity and global climate. The Benguela upwelling system (BUS) is one of the major upwelling areas in the world. Previous reconstructions of the BUS mainly focused on the onset and intensification in southern and central parts, but changes of the northern part have been rarely investigated in detail. Using the Late Miocene to Pliocene organic-walled dinoflagellate cyst record of ODP Site 1081, we reconstruct and discuss the early upwelling history over the Walvis Ridge with a special focus on the movement of the Angola-Benguela Front (ABF). We suggest that during the Late Miocene the Angola Current flowed southwards over the Walvis Ridge more frequently than today because the ABF was probably located further south as a result of a weaker meridional temperature gradient. A possible strengthening of the meridional gradient during the latest Miocene to early Pliocene in combination with uplift of south-western Africa intensified the upwelling along the coast and increased the upwelling's filaments over the Walvis Ridge. An intermediate period from 6.2 to 5.5 Ma is shown by the dominance of *Habibacysta tectata*, cysts of a cool-tolerant dinoflagellate known from the northern Atlantic, indicating changing oceanic conditions contemporaneous with the Messinian Salinity Crisis. From 4.3 Ma on, the upwelling signal got stronger again and waters were well-mixed and nutrient-rich. Our results indicate a northward migration of the ABF as early as 7 Ma and the initial stepwise intensification of the BUS.

Keywords Dinoflagellate cysts · Benguela upwelling · Miocene–Pliocene · Eastern South Atlantic

Introduction

The south-western coast of Africa is currently characterised by cold and nutrient-rich waters related to the occurrence of the Benguela upwelling system (BUS), favouring high primary production. It is one of the major upwelling areas in the world influenced by the global temperature gradient and African orography as well as the surface and deepwater circulation of the South Atlantic. Cold water upwelling in this system is supposed to have initiated in the early Late Miocene (~10–15 Ma) (Siesser 1980; Diester-Haass et al. 1990; Heinrich et al. 2011; Rommerskirchen et al. 2011) during a phase of global cooling. This cooling is part of the transition from a warm and humid variable climate to cooler and drier conditions of the late Neogene driven by changes of the Antarctic ice sheets (Wright et al. 1992; Zachos et al. 2001; Billups and Schrag 2002). Later, the BUS probably played a decisive role in the climate development of the latest Neogene (Etourneau et al. 2012).

Following the mid-Miocene climatic optimum, the re-establishment of major ice sheets in East Antarctica at around 10 Ma led to a globally steepening meridional temperature gradient which would have intensified pressure systems and ocean circulations (Flower and Kennett 1994; Zachos et al. 2001); the South Atlantic Anticyclone (SAA) became stronger and with it the SE trade winds which led to increased upwelling and marine productivity especially

✉ Lydie M. Dupont
dupont@uni-bremen.de; ldupont@marum.de

[1] MARUM - Center for Marine Environmental Sciences, University of Bremen, Leobener Str, Bremen, Germany

[2] School of Environmental Sciences, University of Liverpool, Liverpool L69 7ZT, UK

at around 6.5 Ma (Diester-Haass et al. 2002). These authors hypothesized that the further growth of the Antarctic ice sheets led to a northward migration of the Antarctic Polar Front causing also a shift of the BUS and changing the composition of the water (Diester-Haass 1988; Diester-Haass et al. 1990, 1992). However, recent modelling showed that the introduction of an ice-cap in Antarctica resulted in strong downwelling in the Weddell Sea which attracted warmer water from lower latitudes effectively reducing the meridional sea-surface temperature (SST) gradient in the Atlantic sector of the Southern Ocean. This resulted for the BUS region in slightly reduced Ekman pumping, less upwelling, and warmer subsurface temperatures (Goldner et al. 2013; Knorr and Lohmann 2014; Jung et al. 2014). On the other hand, the ongoing uplift of Southern Africa during the late Miocene and Pliocene (Partridge 1997; Roberts and White 2010) would have strengthened the low-level winds along the southwest African coast (Benguela Jet) enhancing upwelling in the BUS, especially in the central part. A comparison of different model experiments estimates the effects of uplift of Southern Africa on the surface winds driving the BUS far greater than the effects of far field tectonic changes such as the closure of the Central American Seaway or the narrowing of the Indonesian Seaway. However, a subsurface cooling increasing with depth was found in the case of Central American Seaway closure, which indicates the possibility of changing ocean surface conditions in the Benguela region even if upwelling remained constant (Jung et al. 2014). This oceanic cooling is most likely related to a strengthening of the AMOC and hence intensified deep water formation in the Atlantic Ocean with the closure of the Central American Seaway (Zhang et al. 2012).

Generally, the strength and quality of the deepwater formation in the Atlantic Ocean, which is important for the conditions in the BUS, are affected by three gateways along the North Atlantic that underwent considerable changes during the late Miocene: (1) the Central American Seaway, (2) the Greenland-Scotland Ridge overflow and (3) the Mediterranean-Atlantic outflow. Firstly, according to Billups (2002), the closure of the Central American Seaway had influenced the ocean currents between 6.6 and 6 Ma by increasing the Atlantic overturning circulation (AMOC). The influence of the closing of the Central American Seaway on the AMOC is underlined by numerical modelling indicating that the formation of North Atlantic Deepwater (NADW) began when the Central American Seaway had shoaled to a few hundred metres (Butzin et al. 2011). However, the timing of the Central American Seaway closure is strongly debated (Osborne et al. 2014; Sepulchre et al. 2014; Montes et al. 2015). Secondly, changes in the overflow at the Greenland-Scotland Ridge would have increased the proportion of North Atlantic Deepwater (Northern Component Water) as well as strengthen the AMOC for the period between 6 and 2 Ma (Poore et al. 2006). A cooling of Southern Ocean upper circumpolar and intermediate waters affecting the BUS is related to the strengthening of the AMOC (Billups 2002; Poore et al. 2006). Thirdly, dense and salty waters from the desiccating Mediterranean Sea would have increased the AMOC from shortly before 6.2 Ma until 6.0 Ma when the Mediterranean Outflow Water became more and more restricted (Pérez-Asensio et al. 2012; Ivanovic et al. 2014).

A number of palaeostudies focused on the upwelling history of either in the southern and central parts of the BUS or on the ocean side of the Walvis Ridge (Siesser 1980; Diester-Haass et al. 1992; Marlow et al. 2000; Berger et al. 2002b; Udeze and Oboh-Ikuenobe 2005; Heinrich et al. 2011; Rommerskirchen et al. 2011; Rosell-Melé et al. 2014), whereby only ODP Site 1085 in the southern BUS covers its history since the late Miocene (past 14 Ma). ODP Site 1084 in the central BUS area only covers the Pliocene down to ~5 Ma (Marlow et al. 2000; Berger et al. 2002b; Rosell-Melé et al. 2014). These studies indicate that after early initiation in the late Miocene, upwelling increased slowly and mainly at the southern end of the BUS. Upwelling in the central and northern BUS started later, passing through several stages and got intense not until the Pleistocene. With our study on ODP Site 1081 sitting at the northern end of the modern BUS, we complement existing studies focusing on the early Miocene to Pliocene development. The site is sensitive to changes at the northern boundary of the BUS and to movements of the Angola-Benguela Front (ABF). We use a multi-proxy approach to constrain changes in sea-surface conditions between the late Miocene and Pliocene (9–2.7 Ma), with assemblages of organic-walled dinoflagellate cysts as primary proxies, and more particularly to describe changes on the northern edge of the BUS during times of global cooling as well as discuss forcing mechanisms. We complement our results on dinoflagellate cysts with total organic carbon measurements (new and shipboard data) and compare them with alkenone-derived SSTs (Hoetzel et al. 2013). Studies on recent distribution of dinoflagellate cysts along the African coast (e.g. Holzwarth et al. 2007; Marret and Zonneveld 2003; Zonneveld et al. 2013) enable us to associate the oceanographic context (upwelling vs. oligotrophic conditions) with specific cyst assemblages.

The modern Benguela upwelling system

The semi-permanent high-pressure system, the SAA, over the South East Atlantic is the dominating atmospheric feature located at around 32°S 5°W (austral summer) and 27°S 10°W (austral winter) (Petterson and Stramma 1991;

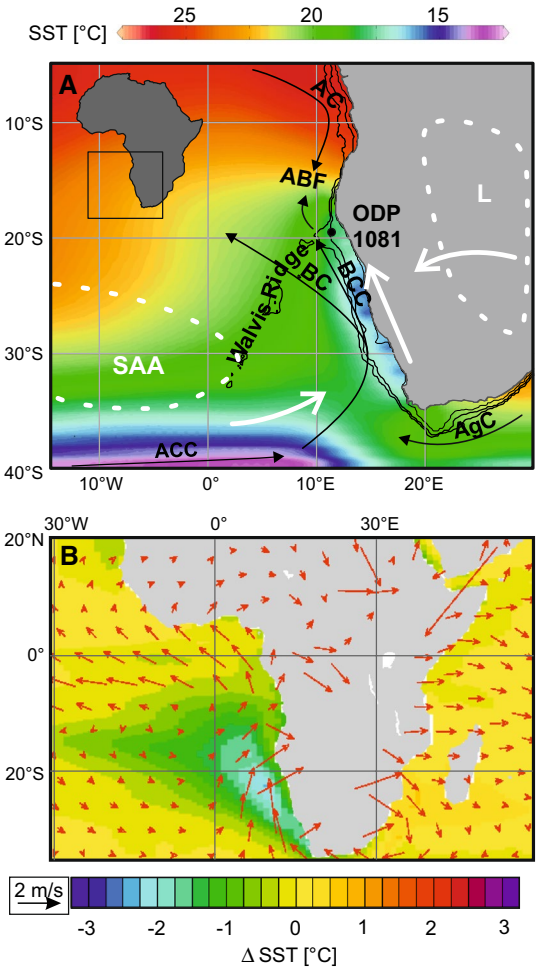

Fig. 1 **a** Map with location of ODP Site 1081 within the South East Atlantic showing the mean annual temperatures in colours (Ocean Data View, U.S. NODC World Ocean Atlas 2009, oceanic features in *black AC* Angola Current, *ABF* Angola-Benguela front, *BC* Benguela current, *BCC* Benguela Coastal current, *ACC* Antarctic Circumpolar current, *AgC* Agulhas current) and main atmospheric features in white (*SAA* South Atlantic Anticyclone, 1020 mbar; *L* low, 1006 mbar). Mean atmospheric sea level pressure cells of January after (Petterson and Stramma 1991). **b** Effect of uplift of Southern Africa on Benguela Upwelling. Changes in surface wind in m/s and sea-surface temperature (SST) in °C calculated from the difference between two runs of the CCSM3 model: one configured with present-day mountain elevation (full) and the other with half present-day elevation (full minus half), after Jung et al. (2014)

Fig. 1). The SAA is driving the Benguela Current which flows northwards along the south-western coast of Africa. The Benguela Current contains water from the eastward flowing cold Antarctic Circumpolar Current, which is linked to the polar front. It also takes up water from the warm Agulhas Current, which is flowing from the Indian Ocean around South Africa. At around 28°S the Benguela Current divides into two separate currents: one following the rotation of the SAA turning west crossing the Atlantic and the other flowing further northwards along the south-western African coast under the name of Benguela Coastal Current. Additionally, the Benguela Coastal Current is linked to the south-easterly trade winds (Petterson and Stramma 1991).

The coastal-parallel winds push the coastal surface waters via Ekman transport offshore inducing the upwelling of cold and nutrient-rich subsurface waters (e.g. Lutjeharms and Meeuwis 1987). The upwelled nutrients allow a vast production of phytoplankton in the photic zone. Eight upwelling cells have been identified, of which the one west of Lüderitz Bay is the strongest persisting all year long resulting in the coldest surface waters of the BUS (Lutjeharms and Meeuwis 1987). Up to 600 km offshore cold upwelled waters from the coastal upwelling areas mix with surface waters and form nutrient-rich filaments (Lutjeharms and Meeuwis 1987; Lutjeharms and Stockton 1987; Summerhayes et al. 1995). Water of these filaments has clearly enhanced nutrient values, lower temperatures and increased primary production.

The Benguela Coastal Current meets the southward-flowing warm and nutrient-poor Angola Current just north of the Walvis Ridge. Together they form the ABF which today is situated between 14°S and 16°S (Meeuwis and Lutjeharms 1990), dependent on the season. In detail, it is not a single front but a couple of fronts arranged in two frontal zones, a northern and a southern one, whereas the latter one has the larger influence on the overall ABF's characteristics (Kostianoy and Lutjeharms 1999). Like the coastal upwelling, the position of the front depends on the SAA; when the meridional pressure gradient is high, the southern front of the ABF is located further north and the ABF is narrower and sharper (Kostianoy and Lutjeharms 1999). Under weakened SAA conditions and resulting weakened winds, the ABF can be located further to the south (Richter et al. 2010) so that warm nutrient-poor water of the Angola Current can penetrate further southward as far as 24°S along the Namibian coast (Meeuwis and Lutjeharms 1990). As a result, the precipitation on the adjacent coast is enhanced (Hirst and Hastenrath 1983; Nicholson and Entekhabi 1987) and can be increased farther inland (Rouault 2003). The phenomenon occurs on inter-annual timescales and is called Benguela Niño for its similarity to the El Niño Southern Oscillation (Shannon et al. 1986).

Materials and methods

The sampled sediment core was retrieved at the Ocean Drilling Program Site 1081 (19°37′S 11°19′E) in 794 m water depth. The site is located on the Walvis Ridge, dividing the Cape Basin from the Angola Basin, 160 km off the Namibian coast (Wefer et al. 1998). Its located just south of the ABF between the Benguela Current and the warm

waters of the Angola Current and is today influenced by filaments of the BUS. The sediment is composed of olive-grey clayey nanofossil ooze and olive-grey to black clays (Wefer et al. 1998). Sedimentation rates were calculated between 2 and 5 cm/ka using an age model based on biostratigraphy, magnetic reversals and magnetic susceptibility (Berger et al. 2002b). Seventy-one samples were taken with ages between 9 and 2.7 Ma and prepared for palynological investigation. The volume of each sample was estimated by water displacement (in ml with an accuracy of 0.5 ml). For decalcification diluted cold HCl (~5 %) was used and afterwards the material was set in cold HF (~20 %) for 2 days to remove silicates. During the HCl treatment, two *Lycopodium clavatum* tablets (Lund University Batch 938934 and 177745) were added containing 10,679 ± 191 and 18,584 ± 371 spores per tablet, respectively. The residuals were sieved over an 8-µm screen under ultrasonic treatment removing particles smaller than 10–15 µm. The cleaned residues were stored in water and mounted in glycerol for investigation under a light microscope using magnifications of 400×, 600× and 1000×. For each sample at least 300 dinoflagellate cysts were identified and counted.

Dinoflagellate cysts were identified using, among others, de Verteuil and Norris (1992), Marret and Zonneveld (2003), De Schepper and Head (2009) and Schreck et al. (2012). *Brigantedinium* spp. include all round brown smooth dinoflagellate cysts. Because *Batiacasphaera micropapillata* has a strong morphological overlap with *B. minuta* and both occur in the samples, we adopted the nomenclature of De Schepper and Head (2008) and Schreck et al. (2012) in treating both species as one complex. Special attention was also given to the distinction between the *B. micropalillata* complex and *Batiacasphaera hirsuta* in personal communication with Jens Matthiessen and Michael Schreck. *Operculodinium centrocarpum* is identified as *O. centrocarpum* sensu Wall and Dale (1966).

Each species was ecologically sorted after its assumed metabolism mechanism (autotroph and heterotroph, Table 1), and a heterotroph/autotroph ratio (H/A) was calculated expressed as ln(H/A). The H/A ratio was chosen over the G/P (Gonyaulacacean/Peridiniacean) ratio as it reflects better the feeding behaviour of whole assemblages (e.g. Verhoeven and Louwye 2013; Bringué et al. 2014). The log-normal transformation is symmetrical around zero and less sensitive to outliers. Percentages were calculated on the total number of dinoflagellate cyst counted. The calculation of the 95 % confidence intervals of the relative abundances is based on a binomial distribution (Maher

Table 1 Identified species ordered after metabolism

Autotrophic species	
Impagidinium	spp.
Impagidinium	sp. 2 of De Schepper and Head (2009)
Impagidinium	*aculeatum*
Impagidinium	*paradoxum*
Impagidinium	*sphaericum*
Impagidinium	*patulum*
Impagidinium	*strialatum*
Operculodinium	spp.
Operculodinium	*centrocarpum* sensu Wall and Dale (1966)
Operculodinium	*israelianum*
Operculodinium	*janduchenei*
Pentapharsodinium	*dalei*
Lingulodinium	*machaerophorum*
Spiniferites	spp.
Spiniferites	*ramosus*
Spiniferites	*mirabilis*
Spiniferites	cf. *mirabilis*
Spiniferites	*membranaceus*
Achomosphaera	spp.
Nematosphaeropsis	*labyrinthus*
Batiacasphaera	*micropapillata*
Batiacasphaera	*hirsuta*
Tuberculodinium	*vancampoae*
Pyxidinopsis	*reticulata*
Habibacysta	*tectata*
Ataxiodinium	*zevenboomii*
Ataxiodinium	*confusum*
Heterotrophic species	
Brigantedinium	spp.
Selenopemphix	*quanta*
Selenopemphix	*nephroides*
Selenopemphix	*brevispinosa*
Selenopemphix	*brevispinosa conspicua* (see Louwye et al. 2004)
Selenopemphix	*armageddonensis*
Trinovantedinium	*glorianum*
Trinovantedinium	*papulum*
Trinovantedinium	*ferugnomatum*
Trinovantedinium	*applanatum*
Lejeunecysta	spp.
Lejeunecysta	*oliva*
Lejeunecysta	*sabrina*
Quinquecuspis	*concreta*
Unknown, further species	
Sumatradinium	*soucouyanatiae*

1972). Accumulation rates of dinoflagellate cysts were calculated by multiplying the sedimentation rate (Berger et al. 2002b) with the cyst concentration per ml, which was calculated based on the known number of *Lycopodium* spores added in the form of tablets.

For 21 samples the total organic carbon (TOC) contents has been determined by decarbonising a sediment aliquot of ~25 mg using 6 N hydrochloric acid before combustion at 1050 °C in a Heraeus CHN–O-rapid elemental analyzer (see Rommerskirchen et al. 2011). This data set is complemented by TOC shipboard data published in Wefer et al. (1998) and shown in Fig. 4.

Results

A total of 36 dinoflagellate cyst taxa were identified whereof the *Brigantedinium* spp. group is the dominant one. In Figs. 2 and 3, the percentages and accumulation rates of the most abundant species are shown. In general,

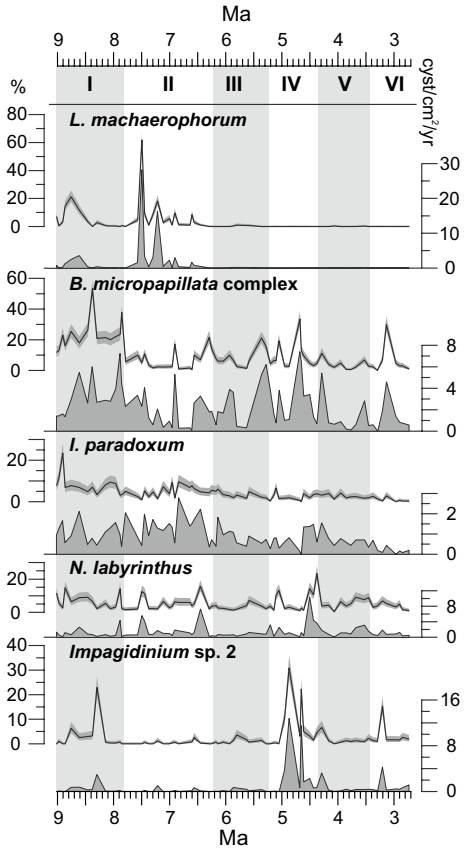

Fig. 2 Relative and absolute abundances of selected dinoflagellate cysts (*L. machaerophorum*, *B. micropapillata* complex, *I. paradoxum*, *N. labyrinthus*, *Impagidinium* sp. 2) within the zoning scheme (*grey boxes*) used in the text. The percentages are shown by *lines* (*left* Y-axes); *shadings* represent 95 % confidence intervals. Accumulation rates are shown by the filled-in *graphs* (*right* Y-axes)

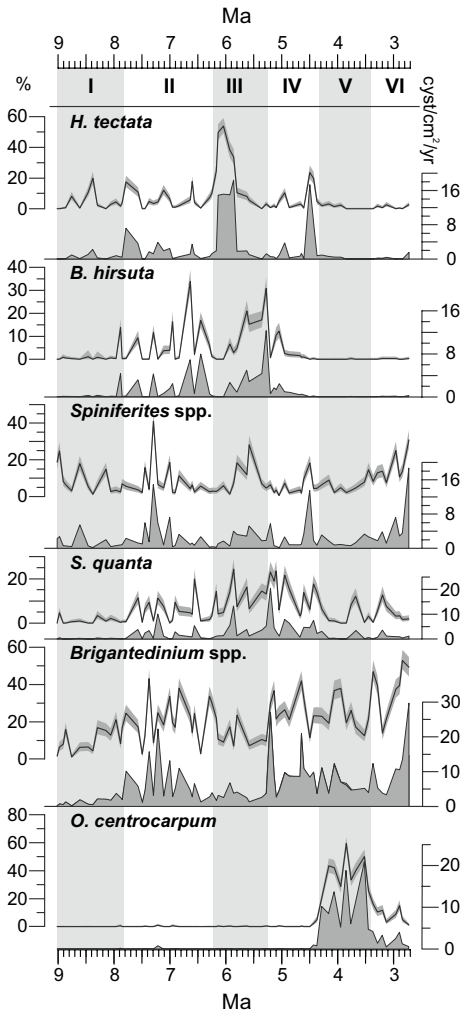

Fig. 3 Relative and absolute abundances of selected dinoflagellate cysts (*H. tectata*, *B. hirsuta*, *Spiniferites* spp., *S. quanta*, *Brigantedinium* spp., *O. centrocarpum*) within the zoning scheme (*grey boxes*) used in the text. The percentages (*left* Y-axes) are shown by *lines*; *shadings* represent 95 % confidence intervals. Accumulation rates are shown by the filled-in *graph* (*right* Y-axes)

both relative and absolute trends show similarity for each species. The record has been visually divided into 6 zones.

Zone I runs from the start of the record at 9–7.8 Ma. This zone is mainly characterized by cysts of the *Batiacasphaera micropapillata* complex with values mostly around 20 % reaching a maximum of 54 %. *Impagidinium paradoxum* is well represented (mean 8 %), especially in the beginning with a peak over 20 %. *Lingulodinium machaerophorum* is present in all samples of Zone I (with two exceptions), reaches 21 % at 8.8 Ma and decreases afterwards to a minor representation in the assemblages (Fig. 2). *Nematosphaeropsis labyrinthus* reaches up to 15 %. *Impagidinium* sp. 2 of De Schepper and Head (2009) cysts are also present (mean 3 %) and have a maximum of 23 % at 8.3 Ma. *Selenopemphix quanta* is only marginally

represented in Zone I. In the beginning of Zone I *Brigantedinium* spp. have generally low values (mean 6 %) that rise at the end of Zone I to 21 %. Almost completely lacking in this interval are *Operculodinium centrocarpum* cysts.

Zone II (7.8–6.2 Ma) is marked by a decline of cyst abundance of the *B. micropapillata* complex to less than 10 % (and less than 5 % around 7 Ma). Additionally, the absolute values are decreasing from around 3 cysts per cm^2 per year to less than 1. Values for *Brigantedinium* spp. and *S. quanta* cysts (Fig. 3) are increased in this zone but show lower values after 7 Ma. Also *H. tectata* decreases from around 17 % to marginal occurrence at 6.5 Ma. However, an increasing trend shows the representation of *B. hirsuta* from low values of less than 10 % to more than 30 %. As in Zone I, *L. machaerophorum* is mostly represented with less than 10 % but peaks at ~7.5 Ma with 63 % of the assemblage. Again *O. centrocarpum* is lacking.

Zone III (6.2–5.3 Ma) is characterized by *H. tectata* cysts dominating the samples until 5.8 Ma and reaching values of 54 %. Additionally, the *S. quanta* curve increases again until 5 Ma. *Spiniferites* spp. and *B. hirsuta* values are also increasing between 6 and 5 Ma.

Zone IV (5.2–4.3 Ma) starts with a drop in *B. hirsuta* curve and a rise of *Brigantedinium* spp. to 42 %. Not present is *L. machaerophorum*. The *B. micropapillata* complex is better represented in the period from 5.2 until 4.2 Ma with a maximum of 34 % (Fig. 2). Between 4.9 and 4.6 Ma *Impagidinium* sp. 2 is well present and peaks twice with values of 23 and 31 %.

Zone V (4.3–3.4 Ma) is defined by the presence of *O. centrocarpum* which is rising from a few per cent at the start of the interval to 60 % at 3.8 Ma.

In Zone VI ranging from 3.4 Ma to the top of the sequence at 2.7 Ma, values of *Brigantedinium* spp., *Spiniferites* spp., and *B. micropapillata* complex rise again.

In Fig. 4, the accumulation rates of summed dinoflagellate cysts are plotted against age. The accumulation rates of cysts range between 7 and 93 cysts per cm^2 per year. One period with lower accumulation rates occurred until 8 Ma, and two periods with generally higher accumulation rates were found between 8 and 6.4 Ma and from 5.4 to 4.2 Ma.

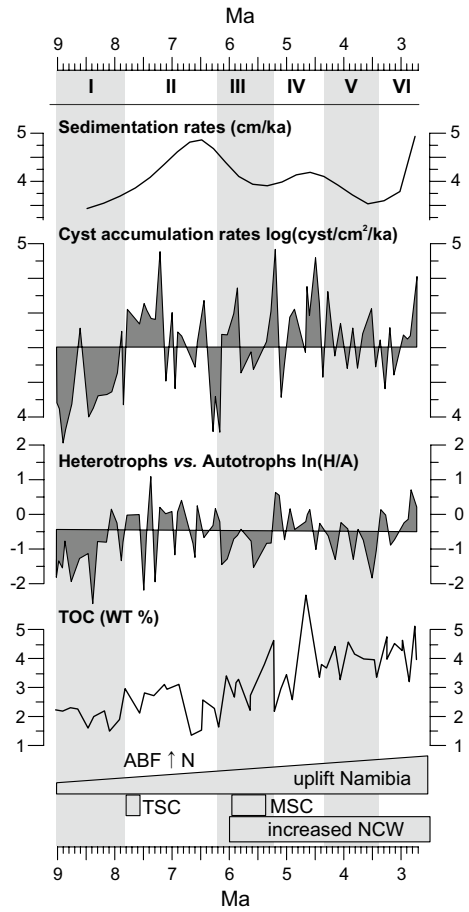

Fig. 4 Sedimentation rates (after Berger et al. 2002b), total dinocyst accumulation rates (cyst/cm^2/yr on a log scale), ratio between heterotroph and autotroph dinoflagellate cysts (ln scale), total organic carbon (TOC in weight percentages after Wefer et al. 1998, complemented by unpublished data of Florian Rommerskirchen). Zoning follows Fig. 2. At the bottom timing of global events that would have influenced sea-surface conditions in the Benguela region; shift of Angola-Benguela Front (ABF) northwards, increased uplift of Namibia since 30 Ma (Roberts and White 2010); timing of the Tortonian Salinity Crisis (TSC) and Messinian Salinity Crisis (MSC) in the Mediterranean (Kouwenhoven et al. 2003; Krijgsman et al. 1999); increased Northern Component Water (NCW) between 6 and 2 after (Poore et al. 2006)

Discussion

Of the 2377 modern motile dinoflagellate species listed worldwide (Gómez 2012), only 10–20 % produce cysts during their life cycle that preserve well in the sediments (Head 1996). The organic-walled cysts found in recent sediments around the world show a distribution that can be related to sea-surface gradients in temperature, salinity, nutrients and sea-ice cover (e.g. de Vernal et al. 1997; Dale et al. 2002; Marret and Zonneveld 2003; Holzwarth et al. 2007; Zonneveld et al. 2001, 2013). Therefore, it has been possible to use them as a tool to reconstruct surface waters conditions, e.g. nutrients and temperature, enabling a record of past upwelling intensity variations. The more important extant species, *L. machaerophorum*, *Impagidinium* spp., *N. labyrinthus*, *O. centrocarpum*, *Brigantedinium* spp., *S. quanta* and *Spiniferites* spp., found at ODP Site 1081 are interpreted after Zonneveld et al. (2013).

The dissolution of cysts sensitive to oxidative degradation (Zonneveld et al. 2001) such as *Brigantedinium* cannot entirely be dismissed, but the relative high abundance of sensitive cysts throughout the record, as well as the

high total concentration values, suggests a minor effect. Therefore, we are confident to use the heterotrophic versus autotrophic ratio (H/A ratio). The H/A ratio (Fig. 4) is used here as an upwelling indicator (Verhoeven and Louwye 2013; Bringué et al. 2014) based on the fact that the autotrophic dinoflagellates are in strong competition with diatoms, whereas the heterotrophic ones feed on diatoms (Smayda and Reynolds 2003). Hence, high H/A ratio values reflect higher production. In most of our record, the ratio is in good concordance to the total dinoflagellate cyst accumulation.

Our results indicate six successive regimes (discussed below): a weak upwelling regime with strong influence of the warm waters of the Angola Current (Zone I, 9–7.8 Ma), an increase of upwelling linked to the intensification of the meridional temperature gradient in combination with Miocene to Pliocene uplift of south-western Africa (Zone II, 7.8–6.2 Ma), a period with exceptional conditions of increasing TOC and warmer SST (Zone III, 6.2–5.3 Ma) during the early stages of the Messinian Salinity Crisis (5.96–5.33 Ma), a resumption of productivity and upwelling after the Messinian (Zone IV, 5.3–4.3 Ma) and further intensification of the upwelling together with the effect of the Cunene River discharge (Zones V and VI, 4.3–2.7 Ma).

The Angola-Benguela front

ODP Site 1081 is located close to the modern position of the ABF, which offers opportunities to record changes in its position since the Miocene. The composition of the dinoflagellate cyst assemblages shows affinity to upwelling conditions over the entire record through nutrient indicating cyst species such as *Brigantedinium* spp., *S. quanta*, *L. machaerophorum* which is in accordance to an initiation of the BUS before 10 Ma (e.g. Siesser 1980; Diester-Haass et al. 1990; Heinrich et al. 2011; Rommerskirchen et al. 2011). However, fluctuations in accumulation rates and relative abundances indicate significant variability in the upwelling during the studied period. Open oceanic species, *Impagidinium paradoxum* (Dale et al. 2002; Zonneveld et al. 2013) and probably *Impagidinium* sp. 2 are stronger represented in Zones I and II (9–6.2 Ma) suggesting warmer and less nutrient-rich environments. Before 7.8 Ma the *B. micropapillata* complex is well represented. Unfortunately, the ecological background of the extinct *B. micropapillata* complex is uncertain. An alkenone-derived SST record indicates warm temperatures of around 26–27 °C for Zone I (Hoetzel et al. 2013). During the early part of the record upwelling conditions were probably rather weak, which is also indicated by low TOC values (Fig. 4; Wefer et al. 1998), and the influence of warm waters from the Angola Current (AC) was still strong compared to later periods.

Southward penetration of the AC is also suggested by the presence of *L. machaerophorum* which today is not present in the BUS but in the area of the AC (Holzwarth et al. 2007). *L. machaerophorum* in an inner-neritic setting—which is not the case at ODP Site 1081—has been associated with nutrient input by river discharge (Versteegh and Zonneveld 1994; Bouimetarhan et al. 2009). Although the pollen record of ODP Site 1081 indicates more humid conditions on the continent, specific indicators for river discharge have not been found for the Late Miocene (Hoetzel et al. 2015). Outside the inner-neritic zone, *L. machaerophorum* has been considered an indicator for stratified warm nutrient-rich waters, e.g. after upwelling relaxation (Marret and Zonneveld 2003; Zonneveld et al. 2013, and references therein), suggesting that periods with stratified water conditions were more frequent and/or longer than today. *I. paradoxum* and *N. labyrinthus* which are more frequent in waters around the ABF (Dale et al. 2002; Zonneveld et al. 2013) also may indicate a southern position of the ABF at least 3° of latitude further south than today. At present, the ABF shifts southwards on inter-annual timescales during Benguela Niños (Shannon et al. 1986). Under these special conditions, the waters over the Walvis Ridge receive a contribution of the Angola Current (Petterson and Stramma 1991; Florenchie et al. 2004; Mohrholz et al. 2004; Richter et al. 2010). It is possible that these Benguela Niño events were more common during Miocene times when the SAA and the trade winds were weaker (Rosell-Melé et al. 2014).

Late Miocene upwelling intensification

Between 7.8 and 6.2 Ma (Zone II) dinoflagellate cyst accumulation rates are generally higher suggesting higher productivity, which we interpret as the result of stronger upwelling (Fig. 4). Further support of the intensified upwelling is given by increased heterotrophic dinoflagellate cyst occurrences, such as *Selenopemphix* and *Brigantedinium* (Zonneveld et al. 2001), which is also shown in the increased H/A ratio (Fig. 4). Slightly higher TOC values as compared to the earlier period (Zone I; Fig. 4) underline increased upwelling conditions. In general, a gradual intensification of the southern BUS (ODP Site 1085) is suggested by other authors. Rommerskirchen et al. (2011) showed a strong sea-surface cooling until 6 Ma, and Udeze and Oboh-Ikuenobe (2005) suggested increased upwelling during the Late Miocene based on dinoflagellate cyst analysis. Early during the interval (prior to 7 Ma), periods of weaker upwelling and stronger influence of warmer waters may have occurred over the Walvis Ridge allowing the presence and even the dominance at 7.5 Ma of *L. machaerophorum*. However, while it is likely that the ABF was located further to the south and its temperature gradient weakened,

the influence of the AC seems to disappear towards the end of Zone II, after 7 Ma. This is indicated by the low occurrences of *L. machaerophorum* and the increase in relative cyst abundance of oceanic species such as *I. paradoxum* and the *B. micropapillata* complex. Our data record a northward shift and intensification of the ABF implying a restriction of the AC to latitudes north of 19°S as well as open ocean conditions over the site as early as 7 Ma (contra Rosell-Melé et al. 2014). The SST record (Hoetzel et al. 2013) shows a moderate cooling between 7.8 and 6.2 Ma, and the TOC record shows reduced values towards the end of the period between 6.7 and 6.5 Ma (Fig. 4).

"Exceptional conditions" during the Mediterranean Salinity Crisis

Between 6.2 and 5.8 Ma the record shows dominance of *H. tectata* which is known to be a cool-water-tolerant species mostly of the Pliocene and Pleistocene of the North Atlantic region (Head 1994; Louwye et al. 2004; Versteegh 1997) but also of the Miocene (Head et al. 1989; Jimenez-Moreno et al. 2006). This maximum of *H. tectata* is flanked by two maxima in the occurrence of *B. hirsuta* (6.8–6.4 and 5.6–5.2 Ma), and an earlier maximum of *H. tectata* occurred between 7.8 and 7.6 Ma. Both *H. tectata* and *B. hirsuta* have not yet been described from the BUS area, but they alternatively dominate the assemblages from 6.8 to 5.2 Ma, representing unique conditions which did not exist before or after that period.

De Schepper et al. (2011) showed that *H. tectata* exceeded 30 % of the dinoflagellate cyst assemblages when the reconstructed Mg/Ca sea-surface temperatures were between 10 and 15 °C. Although *H. tectata* has not yet been described from the South Atlantic, it probably represents strong surface water cooling. However, SST estimates of ODP Site 1081 only show a moderate cooling (Hoetzel et al. 2013). According to Vidal et al. (2002), the sedimentation rates at ODP Site 1085 increased between 6.1 and 5.8 Ma which they correlated with the occurrences of strong glacial events. *S. quanta* also increased during that period, indicating a higher nutrient supply suggesting increased upwelling. On the other hand, other heterotrophic taxa (e.g. *Brigantedinium* spp.) have low values, and consequently the H/A ratio is lower than before although some upwelling is suggested by relative high TOC (Fig. 4).

Zone III (6.2–5.3 Ma) coincides mostly with the Messinian Salinity Crisis (5.96–5.33 Ma; Krijgsman et al. 1999). Mediterranean deepwater formation was weakened since 7.2 Ma (Kouwenhoven and Van der Zwaan 2006) although a connection between the Atlantic Ocean and the Mediterranean Sea remained until the later halite phase between 5.61 and 5.55 Ma (Topper and Meijer 2013). The Mediterranean begun to desiccate shortly before 6.2 Ma creating salty and dense waters flowing into the Atlantic and contributing to NADW formation until 6.0 Ma (Pérez-Asensio et al. 2012). Further restriction of the Mediterranean Outflow Water between 6.0 and 5.5 Ma weakened the AMOC, although the effects of the Mediterranean Outflow Water on the AMOC strongly depend on the salinity of the Outflow Water (Ivanovic et al. 2014). An earlier salinity crisis in the Mediterranean occurred during the Tortonian between 7.8 and 7.6 Ma (Kouwenhoven et al. 2003).

For the period from 6.5 to 5.0 Ma, Rommerskirchen et al. (2011) described TEX_{86} temperature estimates from ODP Site 1085 indicating warming of subsurface waters around 6.3 Ma and between 5.6 and 5.2 Ma. They concluded that the subsurface water warming resulted from a downward mixing of heat caused by a weakening of the AMOC and reduced NADW formation related to reduced outflow of salty Mediterranean water. The period of warm subsurface waters at Site 1085 (southern BUS) coincides with the increased representations of *B. hirsuta* (Site 1081), suggesting that the downward mixing affected the quality of upwelled waters at the northern BUS creating special and non-recurring conditions.

Berger et al. (2002a) argued that the quality of the coastal upwelling waters at the BUS is linked to the deep-water circulation and the strength of the NADW. Increasing NADW formation brings, until a critical point, more silica from the Northern Ocean into the Southern Ocean and eventually changes the chemistry of the upwelled waters at the BUS (enabling the Matuyama Diatom Maximum after Lange et al. 1999). Changes of the silica content might have affected dinoflagellates indirectly via ecological competition with algae or other microorganisms or via changes in food supply and sources. The latter one is important for the heterotrophic species since they feed on diatoms, which are highly depending on silica contents.

A further change of the quality of the upwelled waters could be caused by a poleward undercurrent flowing south from the Angola dome along the African margin transporting silica-rich, phosphate-rich and oxygen-depleted waters (Berger et al. 1998) and increasing the fertile thermocline. A strengthening of this undercurrent and a higher silica content of the waters representing a mixing of the intermediate water and this poleward undercurrent is indicated by a radiolarian peak from 5.8 Ma until 5.25 Ma at ODP Site 1085 (Diester-Haass et al. 2002) coinciding with the younger *B. hirsuta* maximum. The peak in radiolarian might explain lower H/A ratios since radiolarian might have competed with heterotrophic dinoflagellates.

Resumption of upwelling

Around 5.6 Ma at ODP Site 1081 and between 5.6 and 5.3 Ma at Site 1085 (Rommerskirchen et al. 2011), maxima

in SST estimates are recorded after which SSTs fluctuated around a cooling trend during the rest of the Pliocene. Resumption of upwelling in the BUS area is also indicated by a sharp increase of *Brigantedinium* spp. around 5.3 Ma corresponding to increased sedimentation rates at ODP Site 1085 (Diester-Haass et al. 2002). Additionally, high H/A ratios and increasing TOC indicate increased primary production at Site 1081 (Fig. 4). After 5.33 Ma, the Gibraltar strait opened and again very salty and dense Mediterranean Outflow Water could re-intensify NADW formation and AMOC (Ivanovic et al. 2014). More important for the intensification of the BUS , however, might have been the uplift of south-western Africa during the Pliocene (Partridge 1997; Roberts and White 2010). Uplift would have strengthened the coastal low-level winds and increased Ekman pumping causing enhanced upwelling (Jung et al. 2014).

Upwelling intensification and river supply

The presence and dominance of *O. centrocarpum* between 4.3 and 3.4 Ma (Zone V), corroborate findings of Udeze and Oboh-Ikuenobe (2005) in the southern BUS and would indicate nutrient-rich and well-mixed waters representing conditions adjacent to strong upwelling and/or river outflow (Dale et al. 2002). Although *O. centrocarpum* is a cosmopolitan species, it occurs in high abundance in the South East Atlantic in vicinity to upwelling areas (Dale et al. 2002; Marret and Zonneveld 2003; Holzwarth et al. 2007; Zonneveld et al. 2013). It is, additionally, well represented in turbulent and well-mixed waters at the boundary of coastal and oceanic waters (Wall et al. 1977; Dale et al. 2002). *L. machaerophorum* is, however, completely absent, indicating that the partly warm stratified conditions of the Miocene have been completely replaced by stronger upwelling, better mixing and cooler conditions. The increase of *Brigantedinium* spp. abundance and the high TOC concentration (between 4 and 5 wt%; Fig. 4) and further decreasing SSTs (Hoetzel et al. 2013) underline nutrient-rich conditions of a strong upwelling after 3.4 Ma.

Between 4.3 and 3.4 Ma, the H/A ratios show minima during dinoflagellate cyst accumulation maxima indicating again a change in the quality of upwelled waters corresponding to a northward shift of diatom assemblages to the central BUS area (Marlow et al. 2000). These changes may be linked to a stronger influence of Antarctic Intermediate Water.

The increase of *Spiniferites* at the end of the record (Zone VI) might be linked to more coastal conditions and river input (Dale et al. 2002). Increased river discharge in the area since 5 Ma as suggested by the occurrence of *Typha* and *Nymphaea* pollen at the same site (Hoetzel et al. 2015) could also explain the earlier high occurrences of *O. centrocarpum*. Increased river discharge would be a result of rerouting of the Cunene River into the Atlantic Ocean leading to desiccation and outflow of the Cunene lake which probably started in the early Pliocene (Hipondoka 2005).

Links to oceanic and global climate change

The intensification of the BUS and the steepening of the temperature gradient over the ABF imply strengthening of SE trade winds and the regional wind maximum (Benguela Jet) along the coast (Nicholson 2010). It should be kept in mind that the period under discussion concerns the early stages of upwelling of the northern BUS and that upwelling further intensified during the Pleistocene (Berger et al. 2002a, b); in this region SSTs dropped by 10 °C during the past 2.5 Ma (Rosell-Melé et al. 2014).

Prior to 8 Ma, sub-Antarctic stable oxygen isotope values indicate slightly warmer temperatures and less intense glaciations in Antarctica than afterwards (Billups 2002). The temperature gradient over the polar front was probably weaker and situated more southwards and so was the SAA. Additionally, glaciations in the Northern Hemisphere were not yet extensive so that the meteorological equator might have been located further north than today creating a weak meridional temperature and pressure gradient in the Southern Hemisphere (Flohn 1981). A weak meridional temperature gradient would shift the ABF southwards and allow the AC to penetrate southwards over the Walvis Ridge creating Benguela Niño-like conditions (sensu Shannon et al. 1986). Conversely, increase of the meridional gradient (Billups 2002) would have resulted in a northward shift of the ABF, northward migration of the BUS (Diester-Haass et al. 1992), stronger currents and vigorous trade winds. Additionally, Miocene to Pliocene uplift of Southern Africa intensified the near-coastal low-level Benguela Jet and consequently increased upwelling of the BUS (Jung et al. 2014).

The strengthened winds in turn, especially the stronger Benguela Jet, led to aridification of the south-western coast of Africa since warm and humid air from the Atlantic would be hindered to reach large areas of Namibia (Dupont et al. 2013; Hoetzel et al. 2015). Moreover, a stronger Benguela Jet led to intensified upwelling and lower SSTs, which would also act to reduce rainfall (Jung et al. 2014). Dupont et al. (2013) discuss, based on pollen data and deuterium values of plant waxes from ODP Site 1085, that the aridification is caused by a decrease of precipitation derived from the Atlantic and that the main source area of precipitation changed to the Indian Ocean, as is the case today (Gimeno et al. 2010). Miocene to Pliocene mountain uplift would have helped to both strengthen the Benguela Jet and block South Atlantic air from reaching far into the

continent (Jung et al. 2014). The expansion of the grass savanna between 8 and 3 Ma and subsequent expansion of the desert are linked to this aridification (Hoetzel et al. 2013).

The period from 6.8 until 5.2 Ma, in which *H. tectata* and *B. hirsuta* dominate alternatively, forms an interlude in the development of upwelling. It is a period of global oceanic and climate changes contemporaneous to the initiation of the NADW formation (Billups 2002) and the desiccation of the Mediterranean Sea (Krijgsman et al. 1999). Changes in the AMOC and the NADW formation would have resulted in changes of the subsurface waters and thus in the quality of upwelled waters (Berger et al. 2002a), which resulted in a unique flora of the BUS.

From 4.3 Ma on, the intensification of the AMOC and deepwater formation proceeded (Haug and Tiedemann 1998; Steph et al. 2010), changing the intermediate waters of the BUS which again changed the dinoflagellate cyst assemblages. Since ca. 3 Ma the intensification of the Northern Hemisphere glaciations and the introduction to a bipolar icehouse would have shifted the Inter-Tropical Convergence Zone southwards to its average modern position (Billups et al. 1999). The southward shift probably caused an intensified meridional temperature gradient (in the Southern Hemisphere) and further intensification of the low-level winds driving upwelling, which affected the dinoflagellate cyst assemblages.

Summary and conclusions

A record from the Walvis Ridge of organic-walled dinoflagellate cysts in association with total organic carbon data was used to reconstruct changes in Benguela upwelling conditions near its northern boundary, the Angola-Benguela Front. Before SSTs plummeted during the Pleistocene already several phases in upwelling development occurred during late Miocene to early Pliocene. A weak pressure system and an ABF located further south might have resulted in more frequently occurring Benguela Niño conditions before 7.8 Ma. The meridional temperature gradient would have steepened afterwards inducing a northward migration of the ABF and more influence of the Angola Current in the region. This resulted in the occurrence of *L. machaerophorum*, a species blooming in warm stratified nutrient-rich waters after upwelling relaxation. *L. machaerophorum* disappeared from the Benguela upwelling system after 6.5 Ma. Production was high until around 7 Ma and the portion of heterotrophic species was enhanced.

Between 6.8 and 5.2 Ma, *B. hirsuta* and *H. tectata* were abundant during a period with exceptional oceanic conditions probably related to the Messinian Salinity Crisis. *B. hirsuta* occurred during times with relaxed North Atlantic Deepwater production and reduced Atlantic overturning circulation, whereas *H. tectata* occurred during a time of increased NADW production directly before the desiccation of the Mediterranean Basin. The shoaling of the Central American Seaway enhanced NADW production, changing the quality of upwelled waters. Miocene to Pliocene uplift of Southern Africa further increased upwelling of the Benguela upwelling system.

Acknowledgments This work was supported by the DFG Research Center/Cluster of Excellence 'MARUM—The Ocean in the Earth System' and 'GLOMAR—Bremen International Graduate School for Marine Sciences'. The authors thank Michael Schreck and Jens Matthiessen for helping to identify unknown dinoflagellates and discussion about the *Batiacasphaera* complex. Florian Rommerskirchen is thanked for the biogeochemical measurements and Marta Witek for laboratory support. Data are accessible at Pangaea.de.

References

Berger WH, Wefer G, Richter C, Lange CB, Giraudeau J, Hermelin O, Party Shipboard Scientific (1998) The Angola-Benguela upwelling system: paleoceanographic synthesis of shipboard results from Leg 175. In: Wefer G, Berger WH, Richter C et al (eds) Proceedings of the ocean drilling program, initial reports 175. Ocean Drilling Program, College Station, pp 505–531

Berger WH, Lange CB, Pérez ME (2002a) The early Matuyama Diatom maximum off SW Africa: a conceptual model. Mar Geol 180:105–116

Berger WH, Lange CB, Wefer G (2002b) Upwelling history of the Benguela-Namibia system: a synthesis of Leg 175 results. In: Wefer G, Berger WH, Richter C et al (eds) Proceedings of the ocean drilling program, scientific results 175. Ocean Drilling Program, College Station, pp 1–103

Billups K (2002) Late Miocene through early Pliocene deep water circulation and climate change viewed from the sub-Antarctic South Atlantic. Palaeogeogr Palaeoclimatol Palaeoecol 185:287–307

Billups K, Schrag DP (2002) Paleotemperatures and ice volume of the past 27 Myr revisited with paired Mg/Ca and $^{18}O/^{16}O$ measurements on benthic foraminifera. Paleoceanography 17:1003. doi:10.1029/2000PA000567

Billups K, Ravelo AC, Zachos JC, Norris RD (1999) Link between oceanic heat transport, thermohaline circulation, and the intertropical convergence zone in the early Pliocene Atlantic. Geology 27:319–322

Bouimetarhan I, Marret F, Dupont L, Zonneveld K (2009) Dinoflagellate cyst distribution in marine surface sediments off West Africa (17–6°N) in relation to sea-surface conditions, freshwater input and seasonal coastal upwelling. Mar Micropaleontol 71:113–130

Bringué M, Pospelova V, Field DB (2014) High resolution sedimentary record of dinoflagellate cysts reflects decadal variability and 20th century warming in the Santa Barbara Basin. Quat Sci Rev 105:86–101

Butzin M, Lohmann G, Bickert T (2011) Miocene ocean circulation inferred from marine carbon cycle modeling combined with benthic isotope records. Paleoceanography 26:PA1203. doi:10.1029/2009PAOOI901

Dale B, Dale AL, Jansen JHF (2002) Dinoflagellate cysts as environmental indicators in surface sediments from the Congo deep-sea fan and adjacent regions. Palaeogeogr Palaeoclimatol Palaeoecol 185:309–338

De Schepper S, Head MJ (2008) Age calibration of dinoflagellate cyst and acritarch events in the Pliocene—Pleistocene of the eastern North Atlantic (DSDP Hole 610A). Stratigraphy 5:137–161

De Schepper S, Head MJ (2009) Pliocene and pleistocene dinoflagellate cyst and Acritarch Zonation of DSDP hole 610A, Eastern North Atlantic. Palynology 33:179–218

De Schepper S, Fischer EI, Groeneveld J, Head MJ, Matthiessen J (2011) Deciphering the palaeoecology of Late Pliocene and Early Pleistocene dinoflagellate cysts. Palaeogeogr Palaeoclimatol Palaeoecol 309:17–32

de Vernal A, Rochon A, Turon J-L, Matthiessen J (1997) Organic-walled dinoflagellate cysts: palynological tracers of sea-surface conditions in middle to high latitude marine environments. Geobios 30:905–920

de Verteuil L, Norris G (1992) Miocene Protoperidiniacean Dinoflagellate Cysts from the Maryland and Virginia Coastal Plain. In: Head MJ, Wrenn JH (eds) Neogene and quaternary dinoflagellate cysts and acritarchs. American Association of Stratigraphic Palynologists Foundation, Dallas, pp 391–430

Diester-Haass L (1988) Sea level changes, carbonate dissolution and history of the Benguela current in the Oligocene-Miocene off Southwest Africa (DSDP Site 362, Leg 40). Mar Geol 79:213–242

Diester-Haass L, Meyers PA, Rothe P (1990) Miocene history of the Benguela current and Antarctic ice volumes: evidence from rhythmic sedimentation and current growth across the Walvis ridge (Deep Sea Drilling project sites 362 and 532). Paleoceanography 5:685–707

Diester-Haass L, Meyers PA, Rothe P (1992) The Benguela current and associated upwelling on the southwest African Margin: a synthesis of the Neogene-Quaternary sedimentary record at DSDP sites 362 and 532. Geol Soc Lond Spec Publ 64:331–342

Diester-Haass L, Meyers PA, Vidal L (2002) The late Miocene onset of high productivity in the Benguela Current upwelling system as part of a global pattern. Mar Geol 180:87–103

Dupont LM, Rommerskirchen F, Mollenhauer G, Schefuß E (2013) Miocene to Pliocene changes in South African hydrology and vegetation in relation to the expansion of C_4 plants. Earth Planet Sci Lett 375:408–417

Etourneau J, Ehlert C, Frank M, Martinez P, Schneider R (2012) Contribution of changes in opal productivity and nutrient distribution in the coastal upwelling systems to Late Pliocene/Early Pleistocene climate cooling. Clim Past 8:1435–1445

Flohn H (1981) A hemispheric circulation asymmetry during Late Tertiar. Geol Rundschau 70:725–736

Florenchie P, Reason CJC, Lutjeharms JRE, Rouault M, Roy C, Masson S (2004) Evolution of interannual warm and cold events in the Southeast Atlantic Ocean. J Clim 17:2318–2334

Flower BP, Kennett JP (1994) The middle Miocence climatic transition: East Antarctic ice sheet development, deep ocean circulation and global carbon cycling. Palaeogeogr Palaeoclimatol Palaeoecol 108:537–555

Gimeno L, Drumond A, Nieto R, Trigo RM, Stohl A (2010) On the origin of continental precipitation. Geophys Res Lett 37:1–7

Goldner A, Huber M, Caballero R (2013) Does Antarctic glaciation cool the world? Clim Past 9:173–189

Gómez F (2012) A checklist and classification of living Dinoflagellates (Dinoflagellata, Alveolata). CICIMAR Oceánides 27:65–140

Haug GH, Tiedemann R (1998) Effect of the formation of the Isthmus of Panama on Atlantic Ocean thermohaline circulation. Nature 393:673–676

Head MJ (1994) Morphology and paleoenvironmnental significance of the cenozoic dinoflagellate genera *Tectatodinium* and *Habibacysta*. Micropaleontology 40:289–321

Head MJ (1996) Modern dinoflagellate cysts and their biological affinities. In: Jansonius J, McGregor DC (eds) Palynology: Principles and Applications. American Association of Stratigraphic Palynologists Foundation, Salt Lake City, pp 1197–1248

Head MJ, Norris G, Mudie PJ (1989) Palynology and dinocyst stratigraphy of the miocene in ODP Leg 105, Hole 645E, Baffin Bay. In: Srivastava SP, Arthur M, Clement B (eds) Proceedings ocean drilling program, scientific results 105. Ocean Drilling Program, College Station, pp 467–514

Heinrich S, Zonneveld KAF, Bickert T, Hm Willems (2011) The Benguela upwelling related to the Miocene cooling events and the development of the Antarctic Circumpolar current: evidence from calcareous dinoflagellate cysts. Paleoceanography 26:PA3209. doi:10.1029/2010PA002065

Hipondoka M (2005) The development and evolution of Etosha Pan, Namibia. PhD thesis, Julius-Maximilian-Universität Würzburg, Germany

Hirst AC, Hastenrath S (1983) Atmosphere-ocean mechanisms of climate anomalies in the Angola-Tropical Atlantic Sector. J Phys Oceanogr 13:1146–1157

Hoetzel S, Dupont L, Schefuß E, Rommerskirchen F, Wefer G (2013) The role of fire in Miocene to Pliocene C_4 grassland and ecosystem evolution. Nat Geosci 6:1027–1030

Hoetzel S, Dupont LM, Wefer G (2015) Miocene-Pliocene vegetation change in south-western Africa (ODP Site 1081, offshore Namibia). Palaeogeogr Palaeoclimatol Palaeoecol 423:102–108

Holzwarth U, Esper O, Zonneveld K (2007) Distribution of organic-walled dinoflagellate cysts in shelf surface sediments of the Benguela upwelling system in relationship to environmental conditions. Mar Micropaleontol 64:91–119

Ivanovic RF, Valdes PJ, Flecker R, Gutjahr M (2014) Modelling global-scale climate impacts of the late Miocene Messinian salinity crisis. Clim Past 10:607–622

Jimenez-Moreno G, Head MJ, Harzhauser M (2006) Early and middle miocene dinoflagellate cyst stratigraphy of the Central Paratethys, Central Europe. J Micropalaeontol 25:113–139

Jung G, Prange M, Schulz M (2014) Uplift of Africa as a potential cause for Neogene intensification of the Benguela upwelling system. Nat Geosci 7:741–747

Knorr G, Lohmann G (2014) Climate warming during Antarctic ice sheet expansion at the Middle Miocene transition. Nat Geosci 7:376–381

Kostianoy AG, Lutjeharms JRE (1999) Atmospheric effects in the Angola-Benguela frontal zone. J Geophys Res 104:20963–20970

Kouwenhoven TJ, Van der Zwaan GJ (2006) A reconstruction of late Miocene Mediterranean circulation patterns using benthic foraminifera. Palaeogeogr Palaeoclimatol Palaeoecol 238:373–385

Kouwenhoven TH, Hilgen FJ, Van der Zwaan GJ (2003) Late Tortonian-early Messinian stepwise disruption of the Mediterranean-Atlantic connections: constraints from benthic foraminiferal and geochemical data. Palaeogeogr Palaeoclimatol Palaeoecol 198:303–319

Krijgsman W, Hilgen FJ, Raffi I, Sierro FJ, Wilson DS (1999) Chronology, causes and progression of the Messinian salinity crisis. Nature 400:652–655

Lange CB, Berger WH, Lin H-L, Wefer G, Shipboard Scientific Party Leg 175 (1999) The early Matuyama Diatom maximum off SW Africa, Benguela current system (ODP Leg 175). Mar Geol 161:93–114

Louwye S, Head MJ, De Schepper S (2004) Dinoflagellate cyst stratigraphy and palaeoecology of the Pliocene in northern Belgium, southern North Sea Basin. Geol Mag 141:353–378

Lutjeharms JRE, Meeuwis JM (1987) The extent and variability of South-East Atlantic upwelling. S Afr J Mar Sci 5:51–62

Lutjeharms JRE, Stockton PL (1987) Kinematics of the upwelling front off southern Africa. S Afr J Mar Sci 5:35–49
Maher LJJ (1972) Nomograms for computing 0.95 confidence limits of pollen data. Rev Palaeobot Palynol 13:85–93
Marlow JR, Lange CB, Wefer G, Rosell-Melé A (2000) Upwelling intensification as part of the Pliocene-Pleistocene climate transition. Science 290:2288–2291
Marret F, Zonneveld KAF (2003) Atlas of modern organic-walled dinoflagellate cyst distribution. Rev Palaeobot Palynol 125:1–200
Meeuwis JM, Lutjeharms JRE (1990) Surface thermal characteristics of the Angola-Benguela front. S Afr J Mar Sci 9:261–279
Mohrholz V, Schmidt M, Lutjeharms JRE, John H-C (2004) Space-time behaviour of the Angola-Benguela frontal zone during the Benguela Niño of April 1999. Int J Remote Sens 25:1337–1340
Montes C, Cardona A, Jaramillo C, Pardo A, Silva JC, Valencia V, Ayala C, Pérez-Angel LC, Rodriguez-Parra LA, Ramirez V, Niño H (2015) Middle Miocene closure of the Central American Seaway. Science 348:226–229
Nicholson SE (2010) A low-level jet along the Benguela coast, an integral part of the Benguela current ecosystem. Clim Change 99:613–624
Nicholson SE, Entekhabi D (1987) Rainfall variability in Equatorial and Southern Africa: relationships with sea surface temperatures along the Southwestern Coast of Africa. J Clim Appl Meteorol 26:561–578
Osborne AH, Newkirk DR, Groeneveld J, Martin EE, Tiedemann R, Frank M (2014) The seawater neodymium and lead isotope record of the final stages of Central American Seaway closure. Paleoceanography 29:715–729
Partridge T (1997) Cainozoic environmental change in southern Africa, with special emphasis on the last 200,000 years. Prog Phys Geog 21:3–22
Pérez-Asensio JN, Aguirre J, Schmiedl G, Civis J (2012) Impact of restriction of the Atlantic-Mediterranean gateway on the Mediterranean outflow water and eastern Atlantic circulation during the Messinian. Paleoceanography 27:PA3222. doi:10.1029/2012PA002309
Petterson RG, Stramma L (1991) Upper-level circulation in the South Atlantic Ocean. Prog Oceanogr 26:1–73
Poore HR, Samworth R, White NJ, Jones SM, McCave IN (2006) Neogene overflow of Northern Component Water at the Greenland-Scotland Ridge. Geochem Geophy Geosy 7:Q06010. doi:10.1029/2005GC001085
Richter I, Behera SK, Masumoto Y, Taguchi B, Komori N, Yamagata T (2010) On the triggering of Benguela Niños: remote equatorial versus local influences. Geophys Res Lett 37:L20604. doi:10.1029/2010GL044461
Roberts GG, White N (2010) Estimating uplift rate histories from river profiles using African examples. J Geophys Res 115:B02406. doi:10.1029/2009JB006692
Rommerskirchen F, Condon T, Mollenhauer G, Dupont L, Schefuß E (2011) Miocene to Pliocene development of surface and subsurface temperatures in the Benguela Current system. Paleoceanography 26:PA3216. doi:10.1029/2010PA002074
Rosell-Melé A, Martínez-Garcia A, McClymont EL (2014) Persistent warmth across the Benguela upwelling system during the Pliocene epoch. Earth Planet Sci Lett 386:10–20
Rouault M (2003) South East tropical Atlantic warm events and southern African rainfall. Geophys Res Lett 30:8009. doi:10.1029/2002GL014840
Schreck M, Matthiessen J, Head MJ (2012) A magnetostratigraphic calibration of Middle Miocene through Pliocene dinoflagellate cyst and acritarch events in the Iceland Sea (Ocean Drilling Program Hole 907A). Rev Palaeobot Palynol 187:66–94
Sepulchre P, Arsouze T, Donnadieu Y, Dutay J-C, Jaramillo C, Le Bras J, Martin E, Montes C, Waite AJ (2014) Consequences of shoaling of the Central American Seaway determined from modeling Nd isotopes. Paleoceanography 29:176–189
Shannon LV, Boyd AJ, Brundrit GB, Taunton-Clark J (1986) On the existence of an El Niño-type phenomenon in the Benguela System. J Mar Res 44:495–520
Siesser WG (1980) Late Miocene origin of the Benguela upwelling system off Northern Namibia. Science 208:283–285
Smayda TJ, Reynolds CS (2003) Strategies of marine dinoflagellate survival and some rules of assembly. J Sea Res 49:95–106
Steph S, Tiedemann R, Prange M, Groeneveld J, Schulz M, Timmermann A, Nürnberg D, Rühlemann C, Saukel C, Haug GH (2010) Early Pliocene increase in thermohaline overturning: a precondition for the development of the modern equatorial Pacific cold tongue. Paleoceanography 25:PA2202. doi:10.1029/2008PA001645
Summerhayes CP, Kroon D, Rosell-Melé A, Jordan RW, Schrader H-J, Hearn R, Villanueva J, Grimalt JO, Eglinton G (1995) Variability in the Benguela Current upwelling system over the past. Prog Oceanogr 35:207–251
Topper RPM, Meijer PTh (2013) A modeling perspective on spatial and temporal variations in Messinian evaporite deposits. Mar Geol 336:44–60
Udeze C, Oboh-Ikuenobe F (2005) Neogene palaeoceanographic and palaeoclimatic events inferred from palynological data: Cape Basin off South Africa, ODP Leg 175. Palaeogeogr Palaeoclimatol Palaeoecol 219:199–223
Verhoeven K, Louwye S (2013) Palaeoenvironmental reconstruction and biostratigraphy with marine palynomorphs of the Plio-Pleistocene in Tjörnes, Northern Iceland. Palaeogeogr Palaeoclimatol Palaeoecol 376:224–243
Versteegh GJM (1997) The onset of major Northern Hemisphere glaciations and their impact on dinoflagellate cysts and acritarchs from the Singa section, Calabria (southern Italy) and DSDP Holes 607/607A (North Atlantic). Mar Micropaleontol 30:319–343
Versteegh GJM, Zonneveld KAF (1994) Determination of (palaeo-) ecological preferences of dinoflagellates by applying detrended and canonical correspondence analysis to Late Pliocene dinoflagellate cyst assemblages of the South Italian Singa section. Rev Palaeobot Palynol 84:181–199
Vidal L, Bickert T, Wefer G, Röhl U (2002) Late Miocene stable isotope stratigraphy of SE Atlantic ODP Site 1085: relation to Messinian events. Mar Geol 180:71–85
Wall D, Dale B (1966) "Living fossils" in western Atlantic plankton. Nature 211:1025–1026
Wall D, Dale B, Lohmann GP, Smith WK (1977) The environmental and climatic distribution of dinoflagellate cysts in modern marine sediments from regions in the North and South Atlantic Oceans and adjacent seas. Mar Micropaleontol 2:121–200
Wefer G, Berger WH, Richter C, Adams DD, Anderson LD, Andreasen DJ, Brüchert V, Cambray H, Christensen BA, Frost GM, Giraudeau J, Gorgas TJ, Hermelin JOR, Jansen JHF, Lange CB, Laser B, Lin H-L, Maslin M, Meyers PA, Motoyama I, Murray RW, Perez ME, Pufahl PK, Spiess V, Vidal L, Wigley R, Yamazaki T (1998) Site, 1081. In: Wefer G, Berger WH, Richter C et al (eds) Proceedings ocean drilling program, initial reports 175. Ocean Drilling Program, College Station, pp 223–727
Wright D, Miller G, Fairbanks G (1992) Early and Middle Miocene stable isotopes: implications for deepwater circulation and climate. Paleoceanography 7:357–389
Zachos J, Pagani M, Sloan L, Thomas E, Billups K (2001) Trends, rhythms, and aberrations in global climate 65 Ma to present. Science 292:686–693
Zhang X, Prange M, Steph S, Butzin M, Krebs U, Lunt DJ, Nisancioglu KH, Park W, Schmittner A, Schneider B, Schulz M (2012)

Changes in equatorial Pacific thermocline depth in response to Panamanian seaway closure: insights from a multi-model study. Earth Planet Sci Lett 317–318:76–84

Zonneveld KAF, Versteegh GJM, De Lange GJ (2001) Palaeoproductivity and post-depositional aerobic organic matter decay reflected by dinoflagellate cyst assemblages of the Eastern Mediterranean S1 sapropel. Mar Geol 172:181–195

Zonneveld KAF, Marret F, Versteegh GJM, Bogus K, Bonnet S, Bouimetarhan I, Crouch E, de Vernal A, Elshanawany R, Edwards L, Esper O, Forke S, Grøsfjeld K, Henry M, Holzwarth U, Kielt J-F, Kim S-Y, Ladouceur S, Ledu D, Chen L, Limoges A, Londeix L, Lu S-H, Mahmoud MS, Marino G, Matsuoka K, Matthiessen J, Mildenhal DC, Mudie P, Neil HL, Pospelova V, Qi Y, Radi T, Richerol T, Rochon A, Sangiorgi F, Solignac S, Turon J-L, Verleye T, Wang Y, Wang Z, Young M (2013) Atlas of modern dinoflagellate cyst distribution based on 2405 datapoints. Rev Palaeobot Palynol 191:1–197